Pharm Res (2010) 27:2520–2527
DOI 10.1007/s11095-010-0255-y

RESEARCH PAPER

# Pulmonary Gene Silencing in Transgenic EGFP Mice Using Aerosolised Chitosan/siRNA Nanoparticles

Ebbe J. B. Nielsen • Jan M. Nielsen • Daniel Becker • Alexander Karlas • Hridayesh Prakash • Sys Z. Glud • Jonathan Merrison • Flemming Besenbacher • Thomas F. Meyer • Jørgen Kjems • Kenneth A. Howard

Received: 26 April 2010 / Accepted: 19 August 2010 / Published online: 8 September 2010


## ABSTRACT

***Purpose*** This work describes the production and application of an aerosolised formulation of chitosan nanoparticles for improved pulmonary siRNA delivery and gene silencing in mice.

***Methods*** Aerosolised chitosan/siRNA nanoparticles were pneumatically formed using a nebulising catheter and sized by laser diffraction. *In vitro* silencing of aerosolised and non-aerosolised formulations was evaluated in an EGFP endogenous-expressing H1299 cell line by flow cytometry. Non-invasive intratracheal insertion of the catheter was used to study nanoparticle deposition by histological detection of Cy3-labeled siRNA and gene silencing in transgenic EGFP mouse lungs using a flow cytometric method.

***Results*** Flow cytometric analysis demonstrated minimal alteration in gene silencing efficiency before (68%) and after (62%) aerosolisation in EGFP-expressing H1299 cells. Intratracheal catheter administration in mice resulted in nanoparticle deposition throughout the entire lung in both alveoli and bronchiolar regions using low amounts of siRNA. Transgenic EGFP mice dosed with the aerosolised nanoparticle formulation showed significant EGFP gene silencing (68% reduction compared to mismatch group).

***Conclusions*** This work provides a technology platform for effective pulmonary delivery and gene silencing of RNAi therapeutics with potential use in preclinical studies of respiratory disease treatment.

**KEY WORDS** aerosol · chitosan · nanoparticles · pulmonary gene silencing · RNA interference · siRNA

E. J. B. Nielsen · S. Z. Glud · F. Besenbacher · J. Kjems · K. A. Howard (✉)
Interdisciplinary Nanoscience Center (iNANO), University of Aarhus
Aarhus, Denmark
e-mail: kenh@inano.au.dk

E. J. B. Nielsen · S. Z. Glud · J. Kjems · K. A. Howard
Department of Molecular Biology, University of Aarhus
Aarhus, Denmark

J. Merrison · F. Besenbacher
Department of Physics and Astronomy, University of Aarhus
Aarhus, Denmark

J. M. Nielsen
Department of Cardiology, Aarhus University Hospital
Skejby, Aarhus, Denmark

D. Becker · A. Karlas · H. Prakash · T. F. Meyer
Max-Planck-Institute for Infection Biology
Berlin, Germany

## INTRODUCTION

RNA interference (RNAi)-based gene silencing using double-stranded small interfering RNA (siRNA) is a promising molecular medicine approach (1). Enzymatic cleavage of target mRNA by the RNA-induced silencing complex (RISC), selected by complementary base pairing of the recruited antisense strand, has been used for specific silencing of disease-associated genes (2,3).

The therapeutic potential of siRNA, however, is compromised by poor cellular uptake, nuclease instability and renal excretion promoting the development of delivery methods (4,5). Lipid and polymer nanoparticle-based siRNA delivery have shown considerable preclinical success after intravenous (i.v.) administration (6–8); however, the high dose requirement as a consequence of poor circulatory half-life and targeting limits their clinical usefulness.

Direct application onto mucosal surfaces, such as the respiratory epithelium, is an attractive alternative to systemic delivery (7,9,10). The mucosal route reduces nuclease degradation, nanoparticle hepatic clearance and serum-induced aggregation, and facilitates direct contact

with pathogen-infected epithelial cells. Furthermore, mucosal viral infections such as influenza and respiratory syncytial virus (RSV) are ideal candidates for the transient effects offered by RNAi-based therapies. Whilst reduction in influenza titers after i.v. injection with PEI/siRNA formulations (11,12) have been demonstrated, concerns regarding serum-induced aggregation in the lung and limited access to the epithelial surface promote the pulmonary route of delivery.

Intranasal administration of naked siRNA has been used successfully for Heme oxygenase-1 silencing (13) and protection against parainfluenza and RSV (14) in mice. Furthermore, recent phase II clinical trials have been conducted by Alnylam with inhaled naked anti-RSV ALN-RSV01 (www.alnylam.com). Recent attention, however, has been focused towards the development of mucosal delivery systems to maximise the efficacy of pulmonary gene silencing. Lung surfactant InfaSurf (15) and TransIT-TKO (14) have been used; however, toxicity concerns promote the search for safer alternatives.

Our group has previously introduced a nanoparticle system composed of the biocompatible polysaccaride chitosan for mucosal delivery of siRNA (16,17). We have utilised the mucoadhesive and mucopermeation properties of chitosan to demonstrate EGFP silencing in the bronchoepithelium of mice after intranasal administration of chitosan nanoparticles containing EGFP-specific siRNA (17). Inadequate deposition in the conducting airways as a consequence of nasal adherence and possible gastrointestinal clearance restricts the efficiency of intranasal-administered chitosan nanoparticles. This work describes chitosan/siRNA aerosols formed by a nebulising catheter for improved pulmonary delivery and gene silencing. A flow cytometric method is presented for quantitative evaluation of gene silencing in EGFP mouse lungs after intratracheal administration of aerosolised chitosan nanoparticles containing anti-EGFP siRNA. This work provides a technology platform for more effective pulmonary delivery and gene silencing of RNAi therapeutics for potential applications in the treatment of respiratory disease.

## MATERIALS AND METHODS

### Chemicals and siRNA

Chitosan (170 kDa, 84% deacetylation) was prepared by Bioneer A/S (Denmark). EGFP-specific siRNA duplex purchased from Dharmacon (USA) containing the sequences sense, 5′-GACGUAAACGGCCACAAGUUC-3′, and antisense, 3′-CGCUGCAUUUGCCGGUGUUCA-5′-, and EGFP-mismatch sense, 5′-GACGUUAGACUGACAAGUUC-3′, and antisense, 3′-CGCUGAAUCUGACCUGUGGUUCA-5′, were used for nanoparticle characterization studies and EGFP interference work. EGFP-specific siRNA from Dharmacon with a Cy3 fluorophore attached to the 3′-end of the antisense strand was used for *in vivo* lung deposition studies. TransIT-TKO siRNA transfection agent was purchased from Mirus Corp. (USA).

### Formation of Chitosan/siRNA Nanoparticles

Nanoparticles were prepared as previously reported (18). Twenty microlitres of siRNA (250 μM) were added to 1 ml filtered chitosan (800 μg/ml) solution (0.2 M NaAc, pH 5.5) whilst stirring and left for 1 h, N:P ratio 57 (*in vitro* studies) and 23 (*in vivo*) as previously used for intranasal administration (17). Fluorescently labelled nanoparticles (N:P ratio 23) were prepared by addition of 20 μl of Cy3-labelled siRNA (250 μM).

### Photon Correlation Spectroscopy of Nanoparticles

The hydrodynamic size of chitosan/siRNA nanoparticles was determined by photon correlation spectroscopy (PCS) using a Zetasizer Nano ZS (Malvern Instruments, Malvern, UK). PCS was performed at 25°C in sodium-acetate buffer, 0.2 M, in triplicate with sampling time and analysis set to automatic. Particle size is presented as the z-average of three measurements ± std. Aerosolised samples were collected in a 10 ml tube, and particle sizes were measured using PCS.

### Formation and Characterisation of Aerosols

The aerosol for *in vivo* use was formed using an AeroProbe™ nebulising catheter (Trudell Medical Instruments, Canada) set at 20 ms pulse time (5 ms gas delay time) and 2.8 bar and 5 bar on the liquid and gas capillaries, respectively.

### Aerosol Characterisation

Seventy-five pulses of aerosols were collected in a vial to evaluate the amount of solution emitted by a single pulse. The vial was weighed before and after, and the weight was converted into volume (using 1 g/cm$^3$ as the density). This was repeated three times, and the average was calculated for different settings. The average amount of air p. pulse was determined by inserting the catheter through the cap of an inverted water-filled 20 ml tube in a water bath. Seventeen pulses were applied, and the loss of water was correlated to air p. volume by weighing the tube before and after. Laser diffraction analysis was carried out to determine droplet size using a HE-Ne laser (Sympatec Helos 632.8 nm, Windox software 3.4).

### *In Vitro* Transfection

H1299 human lung cancer cells stably expressing EGFP (provided by Dr. Anne Chauchereau, CNRS, France) were seeded in 24-well plates at a concentration of $4\times10^5$ cells/ml in RPMI media containing 10% foetal bovine serum (FBS), 1% penicillin and streptomycin and 0.5% G418 and kept at 37°C (with 5% $CO_2$), resulting in $1\times10^5$ cells per well. TransIT-TKO/siRNA formulations were prepared according to the manufacturer's protocol. Transfections were carried out at a siRNA concentration of 50 nM per well in a 250 µl well volume. After 4 h the wells were washed, and 1 ml of fresh media was added. After an additional 44 h the cells were harvested and fixed using 1% paraformaldehyde phosphate-buffered saline (PBS). FACS analysis was performed on a Becton–Dickinson FACSCalibur flow cytometer. FSC/SSC plots were used to determine the main cell population, and a histogram of the FL-1 channel (green channel) was used to determine the mean EGFP fluorescence. Data analysis was performed using CellQuest Pro software.

### Cytotoxicity Assay

H1299 green cells were seeded at a density of $1\times10^5$ cells/well in a 96-well plate in a total well volume of 100 ml of RPMI media containing 10% foetal bovine serum (FBS), 1% penicillin and streptomycin and 0.5% G418 and kept at 37°C (with 5% $CO_2$). Transfections with either chitosan/siRNA nanoparticles or TranslT-TKO were carried out as described above, and cellular cytotoxicity of was determined after 44 h using a tetrazolium-based viability assay (CellTiter 96® $AQ_{ueous}$ One Solution Cell Proliferation Assay (MTS) (Promega)).

#### *In Vivo Deposition*

C57BL/6 mice ($n=4$) were anesthetised with 5% isoflurane and dosed with chitosan nanoparticles containing Cy3-labelled siRNA. For intratracheal administration, the mice were placed on their backs on a slightly inclining support, and the tracheal opening was visualised with a surgical microscope by gently moving the tongue to one side by the use of a pair of blunted tweezers as described previously (19). The catheter tip was then inserted below the vocal cords, and 2 pulses (2 µl each) of particles (N:P 23) were applied. The mice were sacrificed by cervical translocation within 5 min of dosing and immediately perfused fixed with 4% formalin in PBS. Lungs were dissected, immersed in 4% formalin and paraffin embedded. For instranasal administration, animals were placed on their backs, and drops of particle solution (N:P=150) were placed over each nostril. Animals were dosed (30 µl) on day 1 and 3 (total siRNA dose 0.6 µg) and 48 h after dosing were sacrificed by cervical translocation and immediately perfused fixed. For intratracheal administration, the restricted volume capacity of the mouse lung limited the delivered volume compared to intranasal dosing, so a lower N:P ratio was used to ensure similar siRNA content in the dose.

Sections were visualised using an upright fluorescent microscope (Olympus BX 51, Tokyo, Japan) and an inverted Axiovert 200 M fluorescent microscope (Zeiss, Germany) mounted with a high-resolution CoolSnap HQ CCD camera (Photometrics, USA).

#### *In Vivo Transfection*

EGFP-expressing B6;129P2- RAGE tm1.1 mice (transgenic green mice) (Bernard Arnold, DKFZ, Germany) (20) ($n=5$) separated into 4 groups (non-treated, naked EGFP siRNA, nanoparticle/EGFP-specific siRNA and nanoparticle/siRNA mismatch) were used. Animals were anesthetised by an intraperitoneal injection of Xylazin (16 mg/kg body weight)/Ketamin (120 mg/kg body weight) and dosed on day 1 and 3 (0.26 µg of siRNA p. dose) by the catheter intratracheal insertion method as described above. Animals were sacrificed and lung tissue harvested on day 5.

#### *Processing of Tissue and Flow Cytometry*

Lungs were immediately stored on ice in 1.0 ml HBSS buffer containing 10% FCS. The organs were homogenised by pressing the organ through a 30 µm cell mesh with the plunger of a 5 or 10 ml syringe, the red blood cells lysed using erythrocyte lysis buffer (Qiagen), washed three times with PBS containing 0.5% BSA and fixed in PBS containing 1.0% formaldehyde. Fixed homogenates were washed with PBS containing 0.5% BSA and stored at 4°C until FACS analysis. Directly before FACS analysis the samples were filtered (30 µm CellTrics, partec, Munster, Germany). The analysis was performed using a FACS Calibur (BD) flow cytometer and data analysed using Cell Quest Pro and FCS Express V3. Non-treated C57BL/6 mice and transgenic green mice were used to define settings and non-compensated data acquired in a FL-1H/FL-2H (515–545 nm/563–607 nm) dot plot. Cells derived from an non-treated EGFP-expressing mouse were defined as EGFP-positive if the respective population did not overlap with cells derived from a C57BL/6 mouse, which were used to define the background fluorescence. The respective EGFP-positive population (high EGFP fluorescence) was selected and displayed in a FSC/SSC scatter plot, and a homogenous population was selected that showed EGFP fluorescence clearly distinct from background fluorescence. The analysis was done in an FL-1H histogram. The EGFP-positive cells are subdivided into two distinct populations

that were analysed together. To quantify the knockdown, two markers were defined, one encompassing the EGFP-negative population, the second the EGFP-positive populations. The ratio of the overall fluorescence of these two populations was calculated: $R$=(number of events×median FL1H of EGFP-positive population)/(number of events × median FL1H of EGFP-negative population). The ratio of the negative- and positive-defined population is multiplied by the ratio of the events in these populations, thereby taking the biological variance from animal to animal into account. Some animals show generally elevated fluorescence values, and by calculating the ratio, this effect can be cancelled down. The fluorescence ratio is, therefore, a measure of the EGFP-fluorescence with lower values for lower EGFP expression. Approximately 6000 events were counted (EGFP positive population+EGFP negative population).

## RESULTS

### Physicochemical Characterisation

Photon correlation spectroscopy (PCS) was used to measure nanoparticle size before and after aerosolisation to determine if the pneumatic nebulisation process affected particle integrity (Table I). Particle size remained relatively constant after aerosolisation with an acceptable size change of 9% (decreasing from 298 nm to 272 nm). The polydispersity index (PdI) decreased from 0.3 to 0.26 after nebulisation, suggesting an even more narrow size distribution. Increased particle size of 391 nm was measured after incorporation of Cy3-labelled siRNA.

Gas and solution capillary pressure settings for producing small droplet size and volumes suitable for lung deposition in mice were investigated by laser diffraction. Higher solution pressure increased the solution volume being aerosolised p. pulse, but aerosol droplet size also increased. Likewise, increasing the pressure on the gas capillary resulted in a smaller droplet size but concomitant increase in air p. pulse. Five bar gas capillary pressure was, therefore, used to give 900 µl air p. pulse (over 20 ms) acceptable to a mouse lung (21). Narrow size distribution with a mean value of 21.5 µm was obtained at this setting (Table II). Similarly, solution pressure was optimised at 2.8 bar to give a volume of 2.1 µl of particle solution p. pulse (Table II) suitable for intratrachael delivery in mice.

**Table I** Photon Correlation Spectroscopy of Chitosan/siRNA Nanoparticles

| | Size (±std) | Polydispersity index (±std) |
|---|---|---|
| A | 298.1 nm (±7.5) | 0.333 (±0.03) |
| B | 272.3 nm (±1.5) | 0.263 (±0.03) |
| C | 391.8 nm (±3.9) | 0.263 (±0.0) |

A: Chitosan/siRNA, N:P = 23, B: Chitosan/siRNA (Aerosolised), N:P = 23, C: Chitosan/Cy3-siRNA, N:P = 23

### Cellular Studies

EGFP knockdown in EGFP-stably-expressed H1299 cells were performed to evaluate nebulisation effects on nanoparticle-mediated gene silencing (Fig. 1a). Knockdown after incubation with the nanoparticles containing anti-EGFP siRNA was evaluated by flow cytometric analysis. Chitosan/siRNA nanoparticles demonstrated a 68% reduction in fluorescence geometric mean which did not alter significantly after nebulisation (62%). Non-specific knockdown increased from 13% using non-aerosolised mismatch chitosan/siRNA particles to 28% when aerosolised. Commercial TransIT-TKO (81% knockdown efficiency), included as a positive control, also retained knockdown capability after aerosolisation (74%), but non-specific effects were amplified significantly with the mismatch control (60%). TransIT-TKO showed increased cellular cytoxicity compared to the chitosan/siRNA formulation before and after aerosolisation (Fig. 1b). Cells treated with TransIT-TKO exhibited 17% reduced viability compared to untreated cells, whereas chitosan particles had minimal effects on cell viability before (6%) and after (7%) aerosolisation.

### Pulmonary Deposition and RNA Interference

Pulmonary deposition of the nanoparticles was investigated in mice ($n$=4) using intranasal and intratracheal administration. The intranasal method allowed higher doses compared to the intratracheal catheter delivery but is limited due to uncertain dosage reaching the lung as a consequence of gastrointestinal swallowing or nanoparticle adherence in the nasal cavity. The intratracheal catheter insertion allowed a set amount to be delivered directly into the lung, vital for dose response silencing investigation. Comparison of intranasal (Fig. 2a) and intratracheal (Fig. 2b) administration of Cy3-labelled siRNA/chitosan nanoparticles showed an improved distribution in the lungs of mice using the nebulising catheter compared to intranasal route. Particle deposition was observed in the apical region of airway cells both in conducting and the respiratory (alveolar) lung segments.

Evaluation of chitosan/siRNA nanoparticle EGFP knockdown *in vivo* was performed in the transgenic green mouse (Fig. 3) using a quantitative FACS-analysis method.

**Table II** Aerosol Characterization

| Air volume p. Pulse (± std) | Aerosol droplet diameter (±std) | Solution volume p. pulse |
|---|---|---|
| 895 μl (±23) | 21.5 μm (±10) | 2.1 μl |

Settings: Gas Capillary pressure, 5 bar, solution capillary pressure, 40 PSI, Pulse length 20 ms

Four different groups ($n=5$) were chosen (non-treated, naked EGFP siRNA, nanoparticle/EGFP-specific siRNA and nanoparticle/siRNA mismatch). Doses were administered by catheter intratracheal administration on day 1 and 3, animals were sacrificed on day 5, and lungs were immediately prepared for FACS analysis. To quantify the knockdown of EGFP, the fluorescence ratio (R) was used (refer to Materials and Methods). Nanoparticles containing EGFP-specific siRNA were able to reduce the fluorescence ratio compared to the mismatch formulation (37% reduction), naked siRNA (61% reduction) and the non-treated group (82% reduction). There was no significant difference in the fluorescence ratio between naked siRNA and nanoparticle/siRNA mismatch treated mice. The loss of animals is thought to be due to the Xylazin/Ketamin anaesthesia rather than the nanoparticle treatment, confirmed in later deposition studies by lower mortality using alternative isoflurane anaesthesia (data not shown).

## DISCUSSION

This work presents the application of chitosan/siRNA nanoparticle aerosols for improved pulmonary delivery and gene silencing in transgenic EGFP mice. The pneumatic process mediated by a nebulisation catheter was optimised for small droplet size and volumes suitable for lung deposition in mice. Non-invasive intratracheal insertion allowed direct delivery of controlled set amounts of chitosan/siRNA nanoparticles into the lungs required to standardise gene silencing.

The Aeroprobe nebulising system employed for this work has previously been used for pulmonary delivery and gene expression of aerosolised chitosan/DNA and PEI/DNA complexes in mice (22). The invasive surgical procedure used for catheter insertion, however, precludes multiple rounds of dosing required in gene silencing protocols. We, therefore, adapted a non-invasive technique (19) in order to meet this multiple dose requirement.

Aerosolisation of the nanoparticles did not alter the capability to silence endogenous EGFP in H1299 cells, revealed by a 68% knockdown before and 62% knockdown after aerosolisation (Fig. 1a). Interestingly, the commercial aerosolised TransIT-TKO reagent showed significant non-specific EGFP reduction (60%) compared to the aerosolised mismatch chitosan sample (28% knockdown). This difference could be attributed to increased cytotoxity exhibited by TransIT-TKO compared to chitosan samples (refer to Fig. 1b).

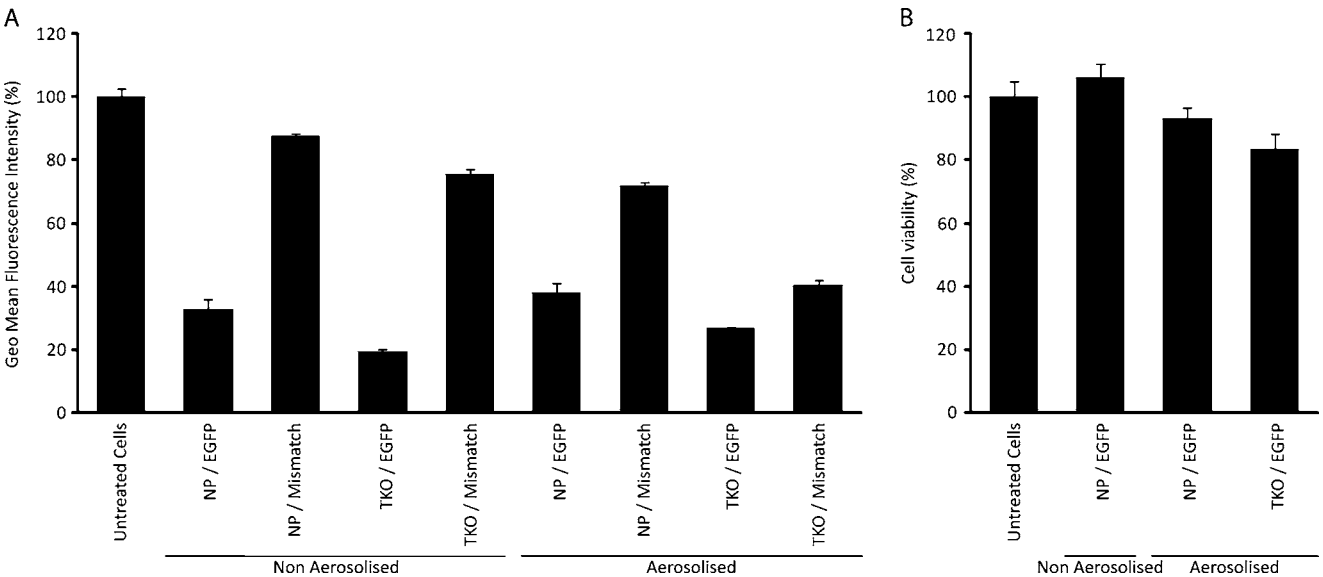


**Fig. 1** **A**: Investigation of the effect of nebulisation process of chitosan/siRNA nanoparticles (NP) on knockdown of EGFP in H1299 cell line. TransIT-TKO/siRNA formulations were used as positive control (4 h transfection, 50 nm siRNA conc. per well). Flow cytometry was used to evaluate EGFP-knockdown based on geometric mean of the fluorescence intensity 48 h after transfection. **B**: Cytotoxicity of NP compared to commercial TransIT-TKO transfection agent with transfection conditions as above.

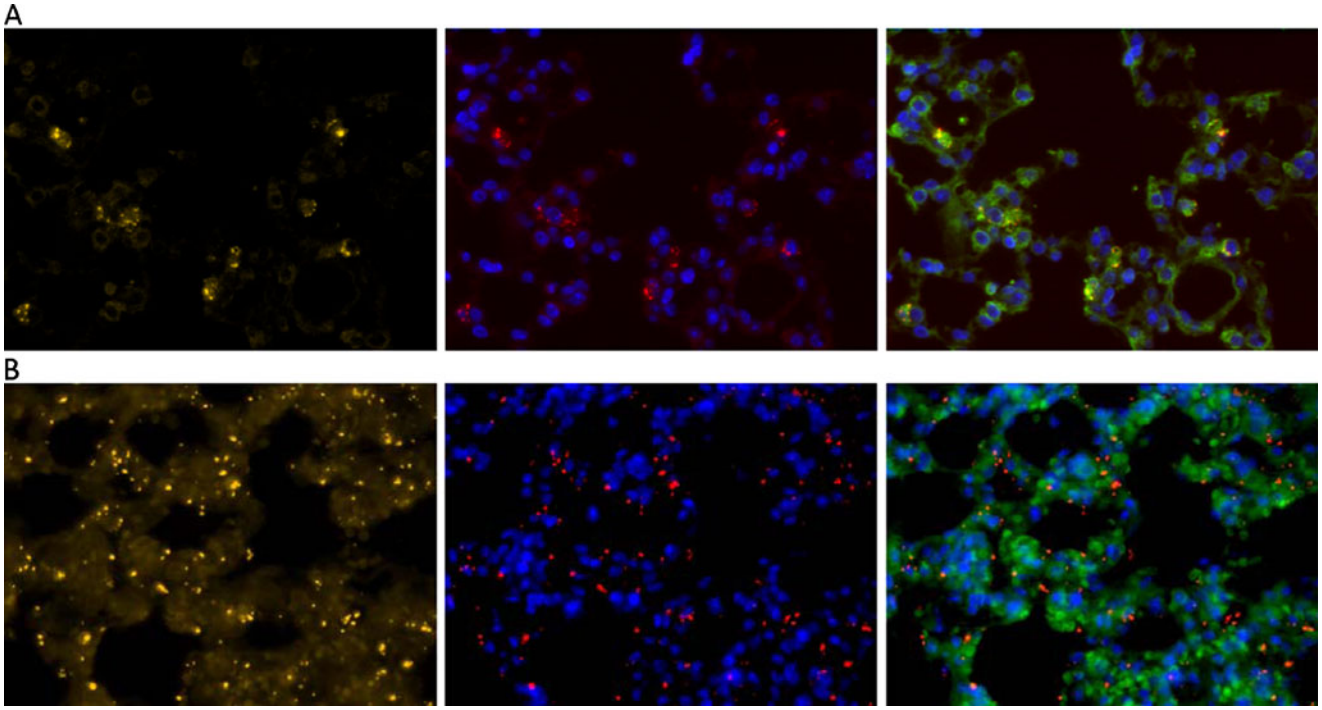


**Fig. 2** Mouse lung deposition of chitosan/siRNA nanoparticle after intranasal (A) and intratracheal aerosol (B) administration (40x). Images show Cy3-labelled siRNA (yellow, left column), Cy3-siRNA (red) and DAPI-labelled nuclei (blue) overlay (middle) and Cy3 (red), DAPI (blue) and EGFP (green) filter overlay (right). **A**: Representative image of alveolar tissue from mice receiving nanoparticle/Cy3-siRNA nanoparticles by nasal instillation (2 doses of ~0.3 $\mu$g). **B**: Representative image showing increased deposition in alveolar tissue of mice receiving aerosolized chitosan/Cy3-siRNA nanoparticles (dose; ~0.26 $\mu$g in 4 $\mu$l). Note: aerosol nanoparticles were also found in the bronchial epithelium.

Particle size is a crucial determinant for cellular uptake either in the bronchial and alveolar epithelial cells or alveolar macrophages. It has been shown that particles with a size of ~200 nm (23) are taken into epithelial cells, whereas larger complexes (~1 µm) are more susceptible to phagocytic capture by alveolar macrophages (24). The size of the non-aerosolised chitosan/siRNA particles used in this work is within the size range suitable for uptake into alveolar and bronchiolar cells. Importantly, the aerosolisation process did not significantly change the size distribution (Table I).

The combination of mucosal epithelia tight junctions and the overlaying mucus layers provides an efficient barrier to nanoparticle uptake. In this work, we aimed to utilise the mucoadhesive (25) and mucopermeable (26) properties of chitosan to improve nanoparticle uptake and gene silencing at mucosal surfaces. In previous studies we have demonstrated EGFP silencing in the bronchoepithelium of transgenic green mice (17) after intranasal administration of chitosan/EGFP-specific siRNA nanoparticles. The requirement for large volumes (50 µl) and high dose (30 µg of siRNA per dose for 5 days) for effective silencing reflect the loss of material during nasal-to-lung transit. Intratracheal insertion of the nebulising catheter in the present work

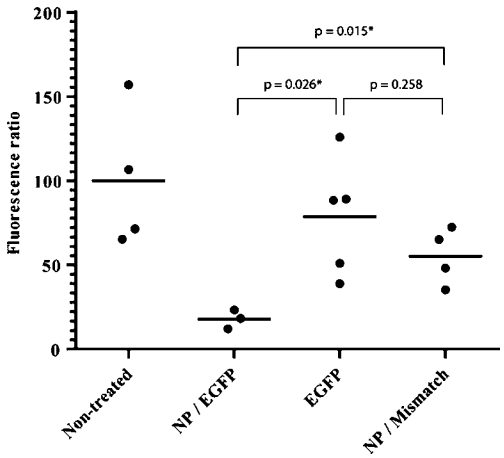


**Fig. 3** Flow cytometric analysis of EGFP knockdown in digested mouse lung after intratracheal administration of aerosolised siRNA formulations in transgenic EGFP mice ($n = 5$, dose; ~0.26 $\mu$g in 4 $\mu$l on day 1 and 3, tissue harvest day 5). The chitosan/EGFP-specific siRNA nanoparticles (NP/EGFP) showed significant knockdown compared to mismatch nanoparticle controls (NP/Mismatch) and naked siRNA (EGFP) determined by lower EGFP fluorescence ratio, $R =$ (Number of events × median FL1-H of EGFP-positive population)/(Number of events × median FL1-H of EGFP-negative population). Normalised to non-treated animals set at 100% fluorescence ratio. Error bars: standard error of the mean. $P$ value denotes students $t$-test ($P < 0.05$) analysis of respective groups, Asterix denotes significant between groups.

increased particle distribution in the alveolar and bronchiolar regions compared to intranasal administration (Fig. 2a, b). Deposition into pathogen-relevant target cells promotes its application for studying RNAi therapeutic effects in pulmonary disease models. Moreover, the delivery of exact siRNA levels into lungs allows a precise investigation into dose-response studies. Furthermore, excess chitosan at N:P ratio 23 is thought to improve particle residence time within the respiratory tract by slowing mucociliary clearance. The particle distribution, however, (Fig. 2b) was seemingly restricted to specific areas, such as the bronchiole and its surrounding alveolar tissue after single administration. It was envisaged that a multiple-dosing and longer-time regime used for the *in vivo* silencing studies would further improve tissue distribution.

Silencing of EGFP in the transgenic green mouse model revealed promising results (37% reduction of fluorescence ratio compared to mismatch group). The observed variance within each group, especially the non-treated group and the group that received the naked siRNA, reflects inherent fluorescence differences in this mouse model.

The flow cytometric technique, however, allows corrections for biological variance to be made using the fluorescence ratio. Furthermore, it is a rapid method of EGFP knockdown evaluation compared to traditional microscopical analysis.

In this work, we demonstrate pulmonary target gene knockdown with low levels (~0.52 μg) of siRNA. Doses ranging from 50 μg (17) to 60–120 μg (11,12) for intravenous injected polycation-based systems have been previously reported. A range from 10 μg (with lung surfactant) (15) to ~40–50 μg (naked siRNA) (13) to 70 μg (both naked and formulated) (14) to 25–100 μg (naked siRNA) (27) has been used for intranasal administration. Furthermore, 75 μg (28) and 100 μg (29) have been used for intratracheal and oral administration, respectively. The ability in our work to study pulmonary gene silencing with low amounts of siRNA reduces the likelihood of RNAi non-specific innate immune induction. This is relevant in light of recent suggestions that anti-viral effects could be attributed to induction of innate immune responses rather than RNAi specificity, dependent on siRNA sequence (30). Gene silencing with such low siRNA amounts is likely due to improved deposition and the effective mucosal delivery capability of the chitosan nanoparticle system.

In this and a previous study (31), we observed minimal pulmonary EGFP reduction in mice treated with naked siRNA. The polyionic nature of siRNA would seemingly restrict cellular uptake; however, several reports have demonstrated pulmonary silencing with naked siRNA (13,14,27). Interestingly, in the study by Glud *et al.* (31), silencing of EGFP in the broncoepithelium was shown with modified naked siRNA after i.v. administration. In contrast, Ge *et al.* (11) observed no reduction in lung viral titres after i.v. admistration of naked anti-influenza siRNA. These observations could reflect differences between target proteins, disease models and dose.

The system presented here is a tool for controlled delivery of set amounts of chitosan/siRNA nanoparticles into the lungs of mice, but future work is focused on development of inhalable formulations. Attention will be given reducing droplet diameters in the range 1–3 μm, optimal for deep lung deposition in humans (32); however, catheter insertion ensures sufficient delivery in the present study. The ability to lyophilise the chitosan/siRNA nanoparticle system whilst retaining silencing activity (18) underlines the potential of these nanoparticles for alternative dry powder inhalable formulations.

This work describes a simple non-invasive method for delivery of chitosan/siRNA nanoparticle aerosols into the lungs of mice. Improved deposition of exact siRNA dosage compared to intranasal administration supports its application for preclinical pulmonary gene silencing studies. The ability of the chitosan/siRNA nanoparticles to silence genes at pulmonary sites shown in this work supports its use for pulmonary RNAi-based therapies.

## ACKNOWLEDGEMENTS

The authors thank Anne Chauchereau for providing the EGFP-expressing H1299 cell line used in this work and Bernard Arnold from DKFZ, Heidelberg, Germany for providing the B6;129P2-RAGE tm1.1 mice. We are also grateful to Helmy Rachman, Kirstin Hoffman and Susan Jackisch for excellent technical assistance with the animal experiments and Uwe Klemm for supervision of the animal work. This work was supported by the Danish Research Council and the EU-FP6 RiGHT programme.

## REFERENCES

1. Fougerolles AR, Vornlocher HP, Maraganore J, Lieberman J. Interfering with disease: a progress report on siRNA-based therapeutics. Nat Rev Drug Discovery. 2007;6:443–53.
2. Wu L, Belasco JG. Let me count the ways: mechanisms of gene regulation by miRNAs and siRNAs. Mol Cell. 2008;29:1–7.
3. Elbashir SM, Harborth J, Lendeckel W, Yalcin A, Weber K, Tuschl T. Duplexes of 21-nucleotide RNAs mediate RNA interference in cultured mammalian cells. Nature. 2001;411:494–8.
4. Gao S, Hansen FD, Nielsen EJB, Wengel J, Besenbacher F, Howard KA, *et al.* The effect of chemical modification and nanoparticle formulation on stability and biodistribution of siRNA in mice. Mol Ther. 2009;17:1225–33.
5. Choung S, Kim YJ, Kim S, Park H, Choi YC. Chemical modification of siRNAs to improve serum stability without loss of efficacy. Biochem Biophys Res Commun. 2006;342:919–27.

6. Fougerolles AR. Delivery vehicles for small interfering RNA *In Vivo*. Hum Gene Ther. 2008;19:125–32.
7. Howard KA. Delivery of RNA interference therapeutics using polycation-based nanoparticles. Adv Drug Delivery Rev. 2009;61:710–20.
8. Wu SY, McMillan NA. Lipidic systems for *in vivo* siRNA delivery. AAPS J. 2009;11:639–52.
9. Howard KA, Kjems J. Polycation-based nanoparticle delivery for improved RNA interference therapeutics. Expert Opin Biol Ther. 2007;7:1811–22.
10. Fougerolles AR, Novobrantseva T. siRNA and the lung: research tool or therapeutic drug? Curr Opin Pharmacol. 2008;8:280–85.
11. Ge Q, Filip L, Bai A, Nguyen T, Eisen HN, Chen J. Inhibition of influenza virus production in virus-infected mice by RNA interference. Proc Natl Acad Sci USA. 2004;101:8676–81.
12. Thomas M, Lu JJ, Ge Q, Zhang C, Chen J, Klibanov AM. Full deacylation of polyethylenimine dramatically boosts its gene delivery efficiency and specificity to mouse lung. Proc Natl Acad Sci USA. 2005;102:5679–84.
13. Zhang X, Shan P, Jiang D, Noble PW, Abraham NG, Kappas A, *et al.* Small interfering RNA targeting Heme Oxygenase-1 enhances Ischemia-Reperfusion-induced lung apoptosis. J Biol Chem. 2004;279:10677–84.
14. Bitko V, Musiyenko A, Shulyayeva O, Barik S. Inhibition of respiratory viruses by nasally administered siRNA. Nat Med. 2004;11:50–5.
15. Massaro D, Massaro GD, Clerch LB. Noninvasive delivery of small inhibitory RNA and other reagents to pulmonary alveoli in mice. Am J Physiol Lung Cell Mol Physiol. 2004;287:1066–70.
16. Liu X, Howard KA, Donga M, Andersen MØ, Rahbek UL, Johnsen MG, *et al.* The influence of polymeric properties on chitosan/siRNA nanoparticle formulation and gene silencing. Biomaterials. 2007;28:1280–8.
17. Howard KA, Rahbek UL, Liu X, Damgaard CK, Glud SZ, Andersen MØ, *et al.* RNA interference *in vitro* and *in vivo* using a chitosan/siRNA nanoparticle system. Mol Ther. 2006;14:476–84.
18. Andersen MØ, Howard KA, Paludan SR, Besenbacher F, Kjems J. Delivery of siRNA from polymeric/siRNA surfaces. Biomaterials. 2008;29:506–12.
19. Benita MB, Zwier R, Junginger HE, Borchard G. Non-invasive pulmonary aerosol delivery in mice by the endotracheal route. Eur J Pharm Biopharma. 2005;61:214–8.
20. Constien R, Forde A, Liliensiek B, Gröne HJ, Nawroth P, Hämmerling G, *et al.* Characterization of a novel EGFP reporter mouse to monitor Cre recombination as demonstrated by a Tie2 Cre mouse line. Genesis. 2001;30:36–44.
21. Valerius KP. Size-dependent morphology of the conductive bronchial tree in four species of myomorph rodents. J Morphol. 1996;230:291–7.
22. Höggård MK, Issa MM, Köhler T, Tronde A, Vårum KM, Artursson P. A miniaturized nebulization catheter for improved gene delivery to the mouse lung. J Gene Med. 2005;7:1215–22.
23. Kato T, Yashiro T, Murata Y, Herbert DC, Oshikawa K, Bando M, *et al.* Evidence that exogenous substances can be phagocytised by alveolar epithelial cells and transported into blood capillaries. Cell Tissue Res. 2003;311:47–51.
24. Rejman J, Oberle V, Zuhorn IS, Hoekstra D. Size-dependent internalization of particles via the pathways of clathrin and caveolae-mediated endocytosis. J Biochem. 2004;377:159–69.
25. Soane RJ, Frier M, Perkins AC, Jones NS, Davis SS, Illum L. Evaluation of the clearance characteristics of bioadhesive systems in humans. Int J Pharm. 1999;178:55–65.
26. Artursson P, Lindmark T, Davis SS, Illum L. Effect of chitosan on the permeability of monolayers of intestinal epithelial cells (Caco-2). Pharm Res. 1994;11:1358–61.
27. Alvarez R, Elbashir S, Borland T, Toudjarska I, Hadwiger P, John M, *et al.* RNA interference-mediated silencing of the respiratory syncytial virus nucleocapsid defines a potent antiviral strategy. Antimicrob Agents Chemother. 2009;53:3952–62.
28. Neira JL, Chung CS, Wesche DE, Perl M, Ayala A. *In vivo* gene silencing (with siRNA) of pulmonary expression of MIP-2 versus KC results in divergent effects on hemorrhage-induced, neutrophil-mediated septic acute lung injury. J Leukocyte Biol. 2005;77:846–53.
29. Perl M, Chung CS, Neira JL, Rachel TM, Biffl WL, Cioffi WG, *et al.* Silencing of Fas, but not Caspase-8, in lung epithelial cells ameliorates pulmonary apoptosis, inflammation, and neutrophil influx after hemorrhagic shock and sepsis. Am J Pathol. 2005;167:1545–59.
30. Robbins M, Judge A, Ambegia E, Choi C, Yaworski E, Palmer L, *et al.* Misinterpreting the therapeutic effects of small interfering RNA caused by immune stimulation. Hum Gene Ther. 2008;19:991–9.
31. Glud SZ, Bramsen JB, Hansen FD, Wengel J, Howard KA, Nyengaard JR, *et al.* Naked siLNA-mediated gene silencing of lung bronchoepithelium EGFP expression after intravenous administration. Oligonucleotides. 2009;19:163–8.
32. Yang W, Peters JI, Williams RO. Inhaled nanoparticles—A current review. Int J Pharm. 2008;356:239–47.